ISSN 1070-3284, Russian Journal of Coordination Chemistry, 2017, Vol. 43, No. 1, pp. 55–62. © Pleiades Publishing, Ltd., 2017.

Thermal Stabilities and Crystal Structures of Two Supramolecular Microporous Frameworks Based on Carboxylate-Dipyridyl Mix-Ligands[1]

L. Y. Xin, F. Y. Ju, X. L. Li, and G. Z. Liu*

College of Chemistry and Chemical Engineering, Luoyang Normal University, Henan, Luoyang, 471022 P.R. China

**e-mail: gzliuly@126.com*

Received October 10, 2015

Abstract—The mix-ligand system of 5-(4-carboxy-2-nitrophenoxy)isophthalic acid (HCn-H_2Ipa) and dipyridyl-type molecule produces two M(II) porous coordination polymers, namely $\{[Zn(HCn\text{-}Ipa)(Dpe)(H_2O)] \cdot 2H_2O\}_n$ (**I**) and $\{[Co(Cn\text{-}HIpa)(Dpe)(H_2O)_3] \cdot 2.5H_2O\}_n$ (**II**) (Dpe = 1,2-di(4-pyridyl)ethylene). Structure determinations reveal that two complexes feature different one-dimensional (1D) polymers assembling into supramolecular microporous frameworks with different thermal stabilities. The 3D supramolecular frameworks of complex **I** show relatively lower stability, which can be caused by relatively larger porous cavity absent of the strong hydrogen bonds interaction, whereas thick-layer blocks in complex **II** are cohered further together by H-bonding interactions to form its 3D supramolecular network with relatively higher stability, indicating extraordinarily stable H-bonding systems; CIF files CCDC nos. 966919 (**I**) and 966920 (**II**).

Keywords: mix-ligand, porous coordination polymers, supramolecular network

DOI: 10.1134/S1070328417010080

INTRODUCTION

The design and assembly of porous coordination polymers (PCPs) have become one of the most active arenas in inorganic and material chemistry during the past several decades [1–5], because the PCPs are potentially applied in guest exchange and separation, gas storage, and selective catalysis, etc. [6–10]. In order to obtain the PCPs, the effective and facile approach for the synthesis of such PCPs is still the appropriate choice of well-designed organic ligands as bridges between ligands and central metal ions to produce porous three-dimensional (3D) networks rely on coordination bonds or intermolecular weak interactions including H-bonds, π–π interactions, and even van der Waals forces. So far, considerable efforts have been devoted to the synthesis of unusual CPs based on carboxylate and/or pyridine-based ligands [11–13].

Among the reported studies, the extended porous frameworks solely generated through the rigid and stronger covalent interactions are well known and extensively investigated. However, it has been demonstrated that the investigation of porous solids produced by the spontaneous aggregation among low-dimensional polymers may be a fascinating subject. It is worth studying in coordination chemistry, and can in concert to create stable molecular networks in crystalline solids that are reproducible, thermally stable, and resilient upon undergoing dynamic processes.

After well-known rigid benzene multicarboxylates as the most typical ligands, conformationally flexible benzene multicarboxylates recently provided access to a vast number of PCPs. Although the diversified conformations of flexible ligand itself sacrifice a measure of control in the design and assembly of PCPs, the flexibility of ligands is also essential to form some desirable porous structures and properties, for example, dynamic solid state materials are probably well-suited for use as "switches," or selective adsorption-desorption agents [14–16]. It is anticipated that supramolecular porous frameworks can exhibit desirable properties in view of their greater structural flexibility compare to those solely formed by the rigid and stronger covalent interactions.

Two representative types of conformationally flexible benzene multicarboxylate lignads were usually chosen in the coordination chemistry: one is benzene carboxylates consisting of long-spanning aliphatic carboxylates with even greater flexiblity; another is "V-shaped" semirigid molecule backbone featuring two benzene rings connected by a nonmetallic atom (C, O, S, or N atoms). Especially, the latter with a compromise in the molecule size and backbone rigidity can provide unique opportunities to succeed in achieving the tunning of the structures and functionality of coordination polymers. In addition, the dipyr-

[1] The article is published in the original.

idyl-type pillar ligands, such as 4,4'-bipyridine (Bipy), 1,2-bi(4-pyridyl)ethane (Bipa), 1,2-di(4-pyridyl)ethylene (Dpe), are known to be ideal connectors between the metal atoms for the propagation of coordination networks and can provide a synergistic coordination together with carboxylate ligands.

Herein, we describe two 1D coordiantion polymers assembled from the mixed ligands of a semirigid "V-shaped" tricarboxylate 5-(4-carboxy-2-nitrophenoxy)isophthalic acid (HCn-H_2Ipa) and dipyridyl-type pillar molecule: $\{[Zn(HCn\text{-}Ipa)(Dpe)(H_2O)] \cdot 2H_2O\}_n$ (**I**) and $\{[Co(Cn\text{-}HIpa)(Dpe)(H_2O)_3] \cdot 2.5H_2O\}_n$ (**II**). Both compounds feature microporous networks based on supramolecular assembly of different 1D chains. The stabilities are investigated in details by the combination of thermogravimetric analysis (TGA) and X-ray powder diffraction (XRPD) techniques.

EXPERIMENTAL

Materials and physical measurements. All the starting materials were of reagent quality and were obtained from commercial sources without further purification. Elemental analysis for C, H, and N were performed on a Vario EL III elemental analyzer. IR spectra were obtained from sample powder pelletized with KBr on an Avatar 360 E.S.P. IR spectrophotometer over a range 4000–600 cm^{-1}. XRPD patterns were recorded with a Rigaku D/Max 3III diffractometer with graphite-monochromatized CuK_α (λ = 1.542 Å) radiation at room temperature. TGA was performed on a STA449C integration thermal analyzer in flowing N_2 with a heating rate of 10 K/min.

Synthesis of I. A mixture of $Zn(OAc)_2 \cdot 2H_2O$ (0.0219 g, 0.10 mmol), HCn-H_2Ipa (0.0347 g, 0.10 mmol), Dpe (0.0182 g, 0.10 mmol) was dissolved in a mixed solvent of EtOH (3.5 mL) and H_2O (3.5 mL) in a 25 mL Teflon-lined stainless steel vessel, which was sealed and heated at 120°C for 4 days under autogenous pressure and then cooled slowly to the room temperature. The colorless blocked crystals were recovered as the pure phase after washing with deionized water, ethanol and acetone, and allowed to dry in air. The yield was 63% (based on Zn).

For $C_{27}H_{23}N_3O_{12}Zn$

anal. calcd, %:	C, 50.13;	H, 3.58;	N, 6.50.
Found, %:	C, 50.44;	H, 3.26;	N, 6.78.

Synthesis of II followed a similar procedure to **I** except that $Co(OAc)_2 \cdot 4H_2O$ was used instead of $Zn(OAc)_2 \cdot 2H_2O$. Pink blocked crystals were collected with a yield of 36% (based on Co).

For $C_{27}H_{28}N_3O_{14.5}Co$

anal. calcd, %:	C, 47.31;	H, 4.12;	N, 6.13.
Found, %:	C, 47.64;	H, 4.01;	N, 6.23.

X-ray structure determination. The crystallographic data collections for complexes **I** and **II** were carried out a Bruker SMART APEX II CCD diffractometer equipped with graphite-monochromated MoK_α radiation (λ = 0.71073 Å) by using the θ–ω scan technique at room temperature. Absorption corrections were based on symmetry equivalent reflections using the SADABS program [17]. The structures were solved by direct methods followed by successive difference Fourier syntheses, and a full-matrix least-squares refinement on $F^2$was carried out using the SHELX-97 program package with anisotropic thermal parameters for all non-hydrogen atoms [18, 19]. All non-hydrogen atoms were easily found from the Fourier difference maps, whereas the H atoms were placed in calculated positions and refined isotropically with a riding model except for water H atoms, which were initially located in a difference Fourier map and included in the final refinement by use of geometrical restraints with O–H 0.85 Å and $U_{iso} = 1.5U_{eq}(O)$. Some disordered solvent H_2O molecules in complexes **I** and **II** are squeezed by PLATON/SQUEEZE program [20]. The details of the structure solutions and final refinements for both complexes are summarized in Table 1. Selected bond distances/angles and hydrogen bonds are listed in Table 2 and Table 3, respectively. Coordination modes of HCn-H_2Ipa ligand observed in complexes **I** and **II** are shown in Scheme 1:

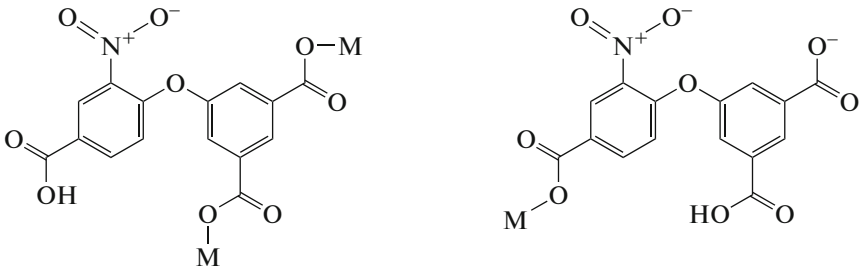

Scheme 1.

Table 1. Crystal and structure refinement data for complexes **I** and **II**

Parameter	Value	
	I	**II**
Empirical-formula	$C_{27}H_{23}N_3O_{12}Zn$	$C_{27}H_{28}N_3O_{14.5}Co$
Fw	646.87	685.46
Temperature, K	296(2)	296(2)
Crystal system	Triclinic	Monoclinic
Space group	$P\bar{1}$	$C2$
a, Å	9.539(4)	26.175(6)
b, Å	11.669(5)	7.5796(16)
c, Å	14.706(6)	16.552(4
α, deg	87.359(5)	90
β, deg	75.984(4)	106.555(2)
γ, deg	83.370(5)	90
Volume, Å ^{3}	1577.4(12)	3147.8(11)
Crystal size, mm	0.38 × 0.17 × 0.15	0.40 × 0.25 × 0.13
Z	2	4
ρ_{calcd}, g cm^{-3}	1.286	1.408
μ, mm^{-1}	0.833	0.614
F(000)	624	1376
θ Range, deg	2.75–25.00	2.57–25.50
Reflections collected	9868	12065
Independent reflections (R_{int})	5340 (0.0399)	5781 (0.0450)
Parameters	372	403
Goodness-of-fit	0.986	1.001
Absolute-structure-parameter		0.020(17)
Final *R* indices ($I > 2\sigma(I)$)	$R_1 = 0.0601$, $wR_2 = 0.1609$	$R_1 = 0.0476$, $wR_2 = 0.1033$
R indices (all data)	$R_1 = 0.0980$, $wR_2 = 0.1753$	$R_1 = 0.0628$, $wR_2 = 0.1119$
Largest diff. peak and hole, *e* Å^{-3}	0.702 and –0.538	0.232 and –0.325

Supplementary materials for two compounds have been deposited with Cambridge Crystallographic Data Centre (nos. 966919 (**I**) and 966920 (**II**); deposit@ccdc.cam.ac.uk or http://www.ccdc.cam.ac.uk/data-request/cif).

RESULTS AND DISCUSSION

Single-crystal X-ray analysis reveals that complex **I** displays a hydrogen-bonded microporous network with the solvent accessible void of ~23.9%. The asymmetric unit contains one crystallographically nonequivalent Zn(II) atom, one Dpe molecule, one double-deprotonated HCn-Ipa dianion, one coordinated H_2O and two disordered guest H_2O molecules which were squeezed. The Zn(II) atom is coordinated by two carboxylate O atoms of Ipa group, one coordinated H_2O, and one Dpe N atom defining a distorted $ZnNO_3$ tetrahedral geometry (Fig. 1a). The Zn–O bond lengths are in the range of 1.935(3)–2.036(4) Å and the Zn–N bond length is 2.025(3) Å.

Table 2. Selected bond lengths (Å) and angles (deg) for compounds **I** and **II***

Bond	*d*, Å	Bond	*d*, Å
		I	
Zn(1)–O(4)$^{\#1}$	1.935(3)	Zn(1)–O(1)	1.951(3)
Zn(1)–N(2)	2.025(3)	Zn(1)–O(10)	2.036(4)
		II	
Co(1)–O(1)	2.031(3)	Co(1)–O(10)	2.070(3)
Co(1)–O(11)	2.115(3)	Co(1)–N(3)$^{\#1}$	2.134(3)
Co(1)–N(2)	2.141(3)	Co(1)–O(12)	2.172(3)
Angle	ω, deg	Angle	ω, deg
		I	
O(4)$^{\#1}$Zn(1)O(1)	118.84(13)	O(4)$^{\#1}$Zn(1)N(2)	131.50(13)
O(1) Zn(1)N(2)	99.30(13)	O(4)$^{\#1}$Zn(1)O(10)	101.18(13)
O(1)Zn(1)O(10)	102.51(13)	N(2)Zn(1)O(10)	98.20(14)
		II	
O(1)Co(1)O(10)	96.12(13)	O(1)Co(1)O(11)	173.05(13)
O(10)Co(1)O(11)	90.45(11)	O(1)Co(1)N(3)$^{\#1}$	93.06(12)
O(10)Co(1)N(3)$^{\#1}$	93.49(12)	O(11)Co(1)N(3)$^{\#1}$	88.77(12)
O(1)Co(1)N(2)	87.85(13)	O(10)Co(1)N(2)	86.40(12)
O(11)Co(1)N(2)	90.32(12)	N(3)$^{\#1}$Co(1)N(2)	179.09(15)
O(1)Co(1)O(12)	86.33(12)	O(10)Co(1)O(12)	177.14(13)
O(11)Co(1)O(12)	87.04(12)	N(3)$^{\#1}$Co(1)O(12)	87.84(12)
N(2)Co(1)O(12)	92.23(13)		

* Symmetry codes: $^{\#1}$ $x + 1, y, z$ (**I**); $^{\#1}$ $x + 1/2, y + 1/2, z$ (**II**).

The ZnO_3N tetrahedra are bridged by both two carboxylates of Ipa groups along the *x* direction via a monodentate coordination mode (Scheme 1a) forming a 1D chain with HCn groups and Dpe molecules as free lateral arms (Fig. 1b). The dihedral angle between two aromatic ring planes of the Cn-HIpa anion is 63.98° due to flexible rotation of central C–O bonds. The four 1D chains are connected by H-bonds between carboxylate O atoms ($O(8)_{Cn}$–H···$O(2)_{Ipa}$, O···O 2.540(5) Å, ∠O···H–O 171°) as well as H-bonds between coordination H_2O and Dpe N atom ($O(10)_w$–H···$N(3)_{Dpe}$, O···N 2.726(5) Å, ∠H–O···N 168°) enclosing a linear channel with free aperture about 4.20 × 8.82 Å^2 (the short O···O distance not including the van der Waals radii, similarly hereinafter), as shown in Fig. 1c. The adjacent channels are adhered together by further H-bonds between coordination H_2O and carboxylate O atoms ($O(10)_w$–H···$O(3)_{Ipa}$, O···O 2.673(5) Å, ∠H–O···O 173°) as well as H-bonds between coordination H_2O and Dpe N atoms ($O(10)_w$–H···$N(3)_{Dpe}$, O···N 2.726(5) Å, ∠H–O···N 168°) producing its entire hydrogen-bonded microporous networks (Fig. 1d). The channels extend along the *x* direction paralleling to the 1D polymeric chains.

Complex **II** exhibits hydrogen-bonded microporous networks with the solvent accessible void of ~13.4%. The asymmetric unit contains one crystallographically nonequivalent Co atom, one Dpe molecule, one double-deprotonated Cn-HIpa dianion, three coordinated waters, and two and a half lattice water (Fig. 2a). The Co^{2+} ion is coordinated by one carboxylate O atom, three coordinated waters, and two Dpe N atoms defining a distorted CoN_2O_4 octahedral geometry. The Co–O bond lengths are in the range of 2.031(3)–2.172(3) Å, the Co–N bond lengths are between 2.134(3) and 2.141(3) Å.

The CoN_2O_4 octahedra are bridged by N atom of Dpe along the *x* direction forming a 1D chain with the carboxylate of Cn group linking to Co center by a monodentate coordination mode (Scheme 1b) and

Table 3. Hydrogen bond distances (Å) and angles (deg) for compounds **I** and **II***

Contact D–H···A	Distance, Å			DHA angle, deg
	D–H	H···A	D···A	
		I		
O(10)–H(2*w*)···N(3)$^{\#2}$	0.85	1.89	2.726(5)	168
O(10)–H(1*w*)···O(3)$^{\#3}$	0.85	1.83	2.673(5)	173
O(8)–H(8)···O(2)$^{\#4}$	0.82	1.73	2.540(5)	171
		II		
O(6)–H(6)···O(14)$^{\#3}$	0.82	1.85	2.664(4)	171
O(10)–H(1*w*)···O(7)$^{\#4}$	0.85	1.87	2.672(4)	156
O(10)–H(2*w*)···O(8)$^{\#5}$	0.85	1.96	2.795(4)	168
O(11)–H(3*w*)···O(13)$^{\#6}$	0.85	1.98	2.770(4))	154
O(11)–H(4*w*)···O(14)$^{\#7}$	0.85	1.99	2.777(5)	154
O(12)–H(5*w*)···O(5)$^{\#2}$	0.82	2.38	3.188(6)	169
O(12)–H(6*w*)···O(2)$^{\#6}$	0.89	1.95	2.709(4)	142
O(13)–H(7*w*)···O(8)$^{\#4}$	0.85	1.92	2.754(4)	163
O(14)–H(8*w*)···O(2)$^{\#7}$	0.85	1.92	2.768(4)	171
O(14)–H(9*w*)···O(7)$^{\#2}$	0.85	1.98	2.774(4)	156

* Symmetry codes for compounds: $^{\#2}$ *x, y, z* + 1; $^{\#3}$ –*x* + 2, –*y* + 2, –*z*; $^{\#4}$ –*x* + 2, –*y* + 1, –*z* + 1 (**I**); $^{\#2}$ *x, y, z* – 1; $^{\#3}$ –*x* + 1/2, *y* + 1/2, –*z*; $^{\#4}$ –*x* + 1/2, *y* + 1/2, –*z* + 1; $^{\#5}$ *x, y, z* + 1; $^{\#6}$ *x, y* + 1, *z*; $^{\#7}$ –*x* + 1, *y*, –*z* (**II**).

HIpa group as free lateral arms (Fig. 2b). The dihedral angle between two aromatic ring planes of the Cn-HIpa anion is 72.29°. The paralleled chains are connected by H-bonds between coordination H_2O and carboxylate O atom of Cn groups ($O(12)_w$–H···$O(2)_{Cn}$, O···O 2.709(4) Å, ∠H–O···O = 142°) forming a layered motif along the *yx* plane (Fig. 2c). Two adjacent anti-paralleled layers are bridged by H-bonds between coordination H_2O and carboxylate O atoms of Ipa groups ($O(10)_w$–H···$O(8)_{Ipa}$, O···O 2.795(4) Å, ∠H–O···O 168°; $O(12)_w$–H···$O(5)_{Ipa}$; O···O 3.188(6) Å, ∠H–O···O 169°) to produce a bilayered block displaying the linear channels with free aperture about 5.82 × 6.63 Å^2 (the short O···O distance), as shown in Fig. 2d. The bilayer blocks are stacked along the *z* direction by a –AAAA– mode and cohered together by H-bonds between coordination H_2O and carboxylate O atoms of Ipa groups ($O(10)_w$–H···$O(7)_{Ipa}$, O···O 2.672(4) Å, ∠H–O···O 156°) producing its 3D supramolecular network (Fig. 2e). In addition, there exist extensive H-bonds between the solvent H_2O being situated at the interlayers and carboxylate O atoms of Ipa groups ($O(11)_w$–H···$O(13)_{Ipa}$, O···O 2.770(4) Å, ∠H–O···O 154°; $O(11)_w$–H···$O(14)_{Ipa}$, O···O 2.777(5) Å, ∠H–O···O 154°; $O(13)_w$–H···$O(8)_{Ipa}$, O···O 2.754(4) Å, ∠H–O···O 165°; $O(14)_w$–H···$O(2)_{Ipa}$, O···O 2.768(4) Å, ∠H–O···O 171°; $O(14)_w$···H–$O(7)_{Ipa}$, O···O 2.774(4) Å, ∠H···O–O 156°). The channels extend along the *y* direction almost perpendicular to the 1D polymeric chains.

The both compounds are further characterized by the IR spectra, which were consistent with their structures as determined by single-crystal X-ray diffraction. The IR spectra of both complexes exhibit several characteristic bands. Broad bands observed in the region of ~3066 to ~3128 cm^{-1} in **I** and **II** represent O–H stretching modes within the HCn-H_2Ipa ligand and ligated or unbound water molecules. In the both compounds, the characteristic bands observed at around 1700 cm^{-1} indicate the incomplete deprotonation of HCn-H_2Ipa ligand. The strong absorptions at 1566, 1341 cm^{-1} for **I** and 1563, 1366 cm^{-1} for **II** are attributed to the asymmetric stretching vibration

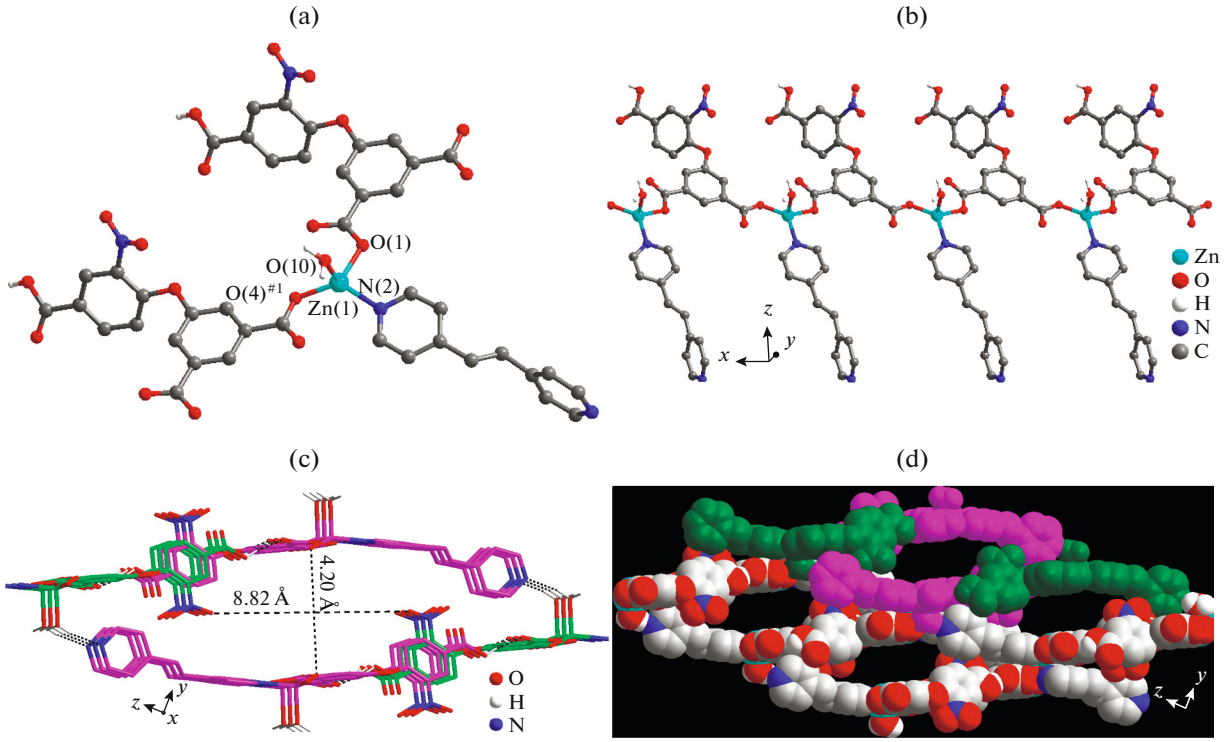

Fig. 1. View of the coordination environment of Zn atoms for **I**. Symmetry codes: $^{\#1}$ 1 + *x*, *y*, *z* (a); view of 1D chain featuring ZnO_3N tetrahedra connected by both two carboxylates of Ipa group for **I** (b); view of a hydrogen-bonded linear channel with free aperture about 4.20 × 8.82 Å^2 enclosed by four 1D chains (c); view of hydrogen-bonded microporous networks (d).

$\nu_{as}(COO^-)$ and the symmetric stretching vibration $\nu_s(COO^-)$, respectively. Medium intensity bands ~1600 and ~1200 cm^{-1} can be ascribed to stretching modes of the pyridyl rings of nitrogen-based ligands. Puckering modes of the pyridyl rings are evident in the region between ~830 and ~670 cm^{-1}.

TGA for complexes **I** and **II** were performed on crystalline samples from room temperature to 800°C under a N_2 atmosphere to investigate their dehydration and degradation behaviors, as shown in Fig. 3. The TGA curves of **I** show that the first weight loss appears at the room temperature with a consecutive weight loss of 8.10% until 177°C, indicating the existence of one ligated water and two disordered guest water per formula unit (calcd. 8.35%) in light of some residual diffraction peaks squeezed by PLATON program. The second weight loss is observed between 226 and 637°C, which is attributed to the decomposition of organic fraction. The final residue is attributed to ZnO component (found 13.07%, calcd. 12.58%). Different from compounds **I**, the supramolecular frameworks of compound **II** are stable up to 90°C. After that, the two and a half lattice water and three ligated water lose (found 14.83%, calcd. 14.44%), and the pyrolysis of the organic ligands over 250°C was observed with a series of consecutive weight losses until the heating end. The final residual species hold a weight of 33.03% of the total sample, which cannot be specifically identified and may be a mixture.

In principle, the stability of an open structure cannot be solely determined from the TGA measurement since it may collapse without a notable change in weight [21], so the XRPD patterns of both complexes were checked at room temperature. The supramolecular porous frameworks of complex **I** are unstable. The open structure can transform in the room temperature, since the XRPD peak positions of complex **I** has appeared change in contrast to the simulate peak positions, and the supramolecular structure further transform to other structure accompany with the increasing temperature. However, the open structures of complex **II** are stable in room temperature, since the peak positions of the simulated and experimental XRPD patterns are in agreement with each other, demonstrating the single phase purity and stability of the products. The difference in intensity may be due to the preferred orientation of the microcrystalline powder samples. In conclusion, The 3D supramolecular frameworks of complexes **I** show relatively lower stability, which can be caused by relatively larger porous cavity absent of the strong hydrogen bonds interac-

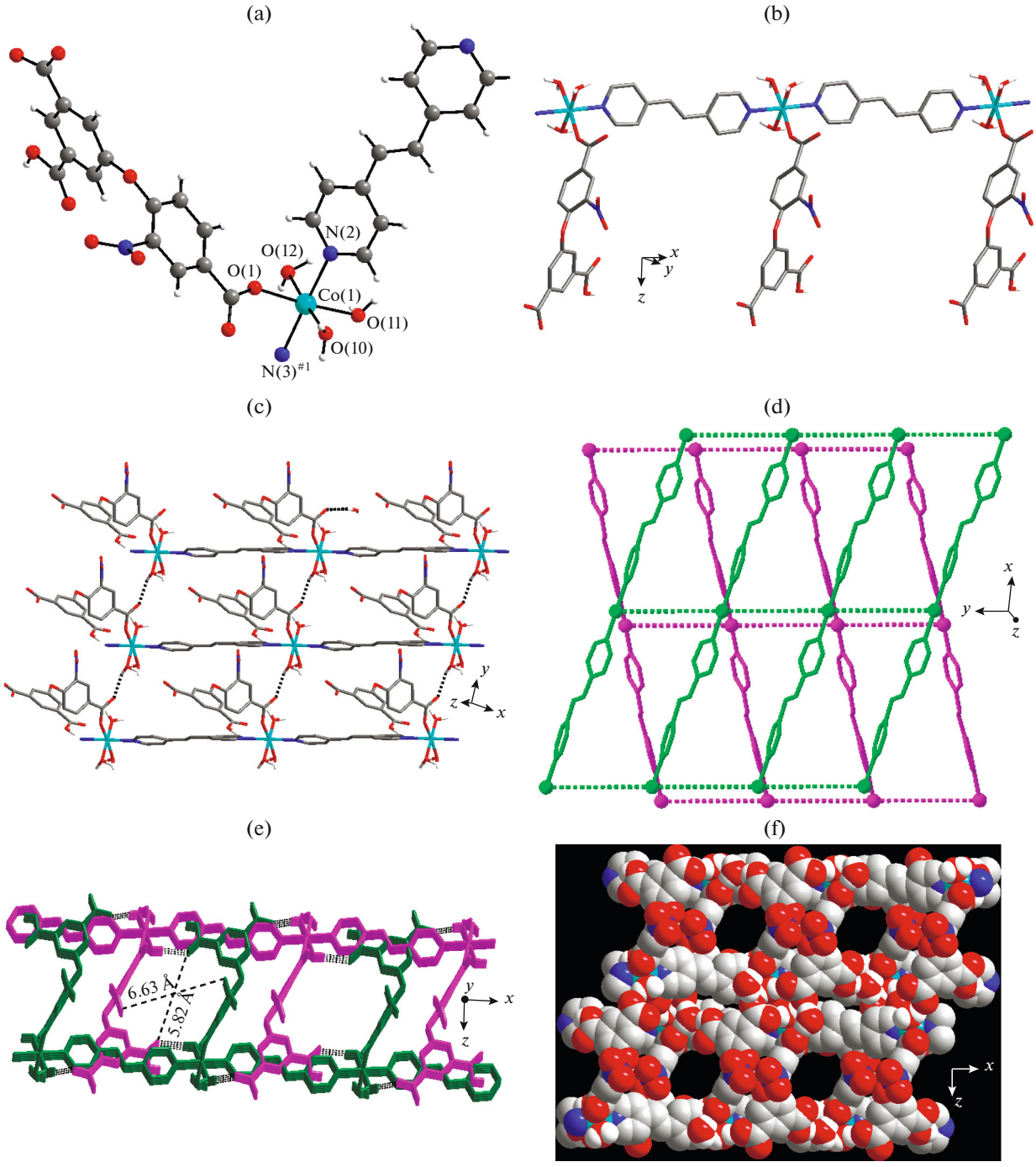

Fig. 2. View of the coordination environment of Co atoms for **II**. Symmetry codes: $^{\#1}$ 0.5 + *x*, 0.5 + *y*, *z* (a); view of a 1D chain featuring Dpe-bridged CoO_4N_2 octahedra for **II** (b); the Co 2D layer and bilayered block in H-bonding interactions (c and d); side view of a thick-layer block consisting of two sheets cohered by H-bonds displaying the linear channels with free aperture about 5.82 × 6.63 Å^2 (e); view of hydrogen-bonding microporous frameworks (f).

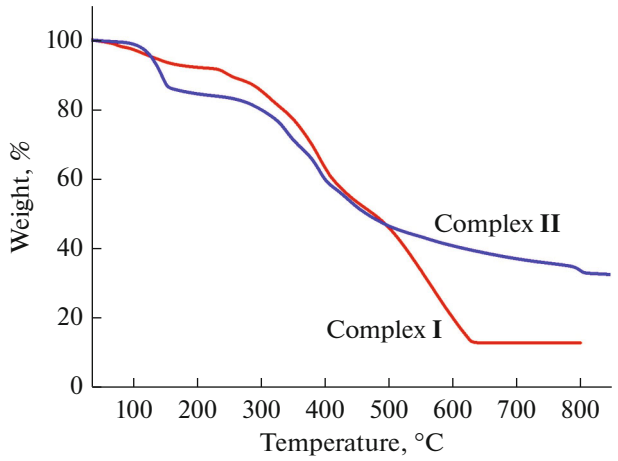

Fig. 3. TGA curve of compounds **I** and **II**.

tion, whereas thick-layer blocks in complex **II** are cohered further together by H-bonding interactions to form its 3D supramolecular network with relatively higher stability, indicating extraordinarily stable H-bonding systems.

ACKNOWLEDGMENTS

This work was supported by the National Natural Science Foundation of China (nos. 21571093 and 21271098), the Program for Science and Technology Innovation Talents in Universities of Henan Province (no. 14HASTIT017), and the Program for Innovative Research Team (in Science and Technology) in University of Henan Province (no. 14IRTSTHN008), the Foundation of Science and Technology of Henan Province (no. 152102310348).

REFERENCES

1. Deng, H.X., Grunder, S., Yaghi, O.M., et al., *Science*, 2012, vol. 336, p. 1018.
2. Cui, Y., Yue, Y., Chen, B., et al., *Chem. Rev.*, 2012, vol. 112, p. 1126.
3. Chae, H.K., Siberio-Perez, D.Y., Kim, J., et al., *Nature*, 2004, vol. 427, p. 523.
4. Xiang, S.C., He, Y.B., Zhang, Z.J., et al., *Nature Commun.*, 2012, vol. 3, p. 954.
5. Luo, X.Z., Jia, X.J., Deng, J.H., et al., *J. Am. Chem. Soc.*, 2013, vol. 135, p. 11684.
6. Gu, Z.Y., Yang, C.X., Chang, N., et al., *Acc. Chem. Res.*, 2012, vol. 45, p. 734.
7. Farrusseng, D., Aguado, S., and Pinel, C., *Angew. Chem. Int. Ed.*, 2009, vol. 48, p. 7502.
8. Jiang, H.L. and Xu, Q., *Chem. Commun.*, 2011, vol. 47, p. 3351.
9. Jiang, G.Y., Wu, T., Bu, X.H., et al., *Cryst. Growth Des.*, 2011, vol. 11, p. 3713.
10. Li, X.L., Liu, G.Z., Wang, L.Y., et al., *CrystEngComm*, 2012, vol. 14, p. 1729.
11. Xin, L.Y., Liu, G.Z., Li, X.L., et al., *Russ. J. Coord. Chem.*, 2013, vol. 39, p. 571.
12. Medishetty, R., Lee, S.S., and Vittal, J.J., *Inorg. Chem.*, 2013, vol. 52, p. 2951.
13. Li, X.L., Liu, G.Z., Xin, L.Y., et al., *Synth. React. Inorg. Met.-Org.* Chem., 2015, vol. 45, p. 914.
14. Dong, X.Y., Zang, S.Q., Song, Y., et al., *J. Am. Chem. Soc.*, 2013, vol. 135, p. 10214.
15. Li, C.P. and Du, M., *Chem. Commun.*, 2011, vol. 47, p. 5958.
16. Liu, G.Z., Li, S.H., Wang, L.Y., et al., *CrystEngComm*, 2013, vol. 15, p. 4571.
17. Sheldrick, G.M., *A Program for the Siemens Area Detector Absorption Correction*, Göttingen: Univ. of Göttingen, 1997.
18. Sheldrick, G.M., *SHELXS-97, Program for X-ray Crystal Structure Determination,* Göttingen: Univ. of Göttingen, 1997.
19. Sheldrick, G.M., *SHELXS-97, Program for X-ray Crystal Structure Refinement,* Göttingen: Univ. of Göttingen, 1997.
20. Spek, A.L., *PLATON, A Multi-Purpose Crystallographic Tool*, Utrecht: Utrecht Univ., 2001.
21. Ma, L.F., Wang, L.Y., Wang, Y.Y., et al., *CrystEngComm*, 2009, vol. 11, p. 109.